

CHROMSYMPO. 1591

IMPROVED SEPARATION SPEED AND EFFICIENCY FOR PROTEINS, NUCLEIC ACIDS AND VIRUSES IN ASYMMETRICAL FLOW FIELD FLOW FRACTIONATION

A. LITZÉN and K.-G. WAHLUND*

Department of Analytical Pharmaceutical Chemistry, University of Uppsala Biomedical Center, Box 574, S-751 23 Uppsala (Sweden)

SUMMARY

The performance of the asymmetrical flow field-flow fractionation channel has been improved by the use of a much thinner (0.12-mm) channel than before and by flow programming (stepwise gradient elution). The thinner channel contributes to a decreased zone broadening which enables complete resolution in a shorter time. Three protein peaks, representing molecular weights from 12 000 to 136 000, were completely resolved within 3 min. Flow programming speeds up the elution of the high-molecular-weight materials which occur late in a fractogram. This enabled separation of a small plasmid fragment (700 base pairs) from the large amounts of a big fragment (4600 base pairs) in 30 min and improved detection of a presumed trimer of albumin. Two viruses ($1.8 \cdot 10^6$ and $50 \cdot 10^6$ daltons) were eluted as narrow peaks within 5 min.

INTRODUCTION

Field flow fractionation (FFF) comprises a group of analytical and micro-preparative separation methods especially suited for macromolecular and particle separations. The basic idea originated with Giddings in 1966¹. Many different modes of FFF have since been described². The flow FFF method used in this work is universal in the sense that it can separate material having a very broad range of molecular weights and particle sizes in one single separation unit. Adjustment of conditions for the actual molecular or particle size is simply made by changing the flow-rates of the cross- and channel-flows. The almost general applicability makes it especially important to develop the performance of flow FFF further. The separation is based on differences in the diffusion coefficients, and the factors which influence separation are thus the molecular and the particle mass and shape. For a more complete list of references to earlier work and a detailed description of the principle the reader is referred to a previous article³.

The type of separations that can be obtained by flow FFF is perhaps best described as a size fractionation, and the results are therefore in a way similar to those of size-exclusion chromatography (SEC). One important aspect in a comparison of flow FFF with SEC is that the former may lack some of the problems observed in the

latter for ultra-high-molecular-weight materials⁴. For example, there is no upper "exclusion limit" in flow FFF (except when the particle size approaches that of the channel thickness) and, if properly designed, elution times in flow FFF may become much smaller than in SEC for a certain resolution level. Theoretical calculations show that the selectivity of flow FFF is superior to that of SEC². This means that there is a potential in flow FFF for better resolution than in SEC if the zone broadening in the flow FFF channel can be kept low enough. A further advantage of flow FFF is that gradient elution can be obtained by programming the flow-rate.

In the previous study³ we obtained much improved resolution and separation speed for proteins by using a thinner channel (0.3 mm). The application of flow FFF was also expanded to new types of compounds, such as the separation of plasmids and plasmid fragments. In the present study we have obtained a further improvement in resolution and speed by using an even thinner channel (0.12 mm). Stepwise flow programming was used to optimize the separation speed. The examples given show rapid separations of proteins and their dimers and trimers, a small plasmid fragment from large amounts of a big fragment, three small plasmid fragments and two plasmids and the isolation of two virus particles.

Very recently, a flow FFF separation system was described in which circular hollow fibres are used as the separation channel instead of the flat, rectangular channel used in our work^{5,6}. The separation appears to be slower in the hollow fibre system.

EXPERIMENTAL

The reader is referred to the authors' previous papers^{3,7} for a detailed description of the construction of the asymmetrical flow FFF channel and its operation. Here, we will note those parts which differ in size or material from those in the previous paper³.

Two channels (I and II) were used, of length 28.5 cm and breadth 1.0 cm. The semipermeable membrane serving as the accumulation wall was a Millipore Type PLGC ultrafiltration membrane (Millipore, Bedford, MA, U.S.A.) with a nominal molecular weight cut-off of 10 000. It consists of a regenerated cellulose membrane on a polypropylene substrate. The two channels differed in their thicknesses, which are determined by the thickness of the spacer material that was clamped between the ultrafiltration membrane and the glass plate serving as the upper wall for the channel. Channel I had a poly(tetrafluoroethylene) (PTFE) spacer with a measured thickness of 0.032 cm. The resulting geometrical volume (void volume) of the channel was 0.87 ml. Channel II had a fluorinated ethylene propylene (FEP) spacer with a measured thickness of 0.012 cm, giving a geometrical volume of 0.35 ml. Calculation of the void time was based on the geometrical volume. The real void volume of a channel may be somewhat smaller than that calculated from the thickness of the spacer. This depends on the compression of that part of the membrane which is covered by the spacer. The values of the void time reported may therefore be somewhat overestimated.

Sample loops were 10 or 98 μ l in volume. The carrier inlet flow was delivered by a Gynkotek constant-flow pump, Model 600/200, Version 600 (Gynkotek, Munich, F.R.G.). The eluate composition was monitored by a Spectromonitor III spectrophotometric detector (Laboratory Data Control, Riviera Beach, FL, U.S.A.) set at 280 nm for proteins and 260 nm for DNA (plasmids, plasmid fragments) and viruses.

Flow programming was performed by manually stepping the needle valve N2 or N3 (see ref. 3), which causes the ratio \dot{V}_c/\dot{V}_{out} to change.

Human serum albumin fraction V, fatty acid-free, and cytochrome *c* from horse heart Type III were obtained from Sigma (St. Louis, MO, U.S.A.). Ferritin and thyroglobulin were from a gel filtration calibration kit (Pharmacia, Uppsala, Sweden). The plasmids were gifts from the Department of Pharmaceutical Microbiology, University of Uppsala (Uppsala, Sweden) and Pharmacia Biotechnology (Uppsala, Sweden). Purified samples of Satellite tobacco necrosis virus (STNV) and Semliki forest virus (SFV) were gifts from the Department of Molecular Biology, University of Uppsala.

The carrier was a Tris-HNO₃ buffer (pH 7.4), ionic strength 0.1, containing 0.02% sodium azide and 1 mM EDTA.

RESULTS AND DISCUSSION

The experimental procedures were as described in previous papers^{3,7} for an asymmetrical flow FFF channel. The same symbols, describing the operating conditions, have been used here: z' = focusing point (distance from channel inlet end); \dot{V}_c = cross-flow-rate during relaxation; \dot{V}_e = cross-flow-rate during elution; \dot{V}_{out} = flow-rate at channel outlet end; \dot{V}_{in} = flow-rate at channel inlet end; t_0 = void time; t_R = retention time; $R = t_0/t_R$ = retention ratio.

Sample injection, channel thickness, retention time and zone broadening

Sample injections were made by the so-called "downstream central sample injection" method, presented in our previous paper³. Thus, the elution of a compound starts from the focusing point, z' , at which the sample was loaded, relaxed and concentrated.

Experiments were performed in two channels, one having a nominal thickness of 0.032 cm, the other 0.012 cm.

The cross-flow-rate during elution determines the retention level of the sample. The higher the cross-flow-rate used, the higher will be the degree of retention, *i.e.*, the lower will be the retention ratio, R . The retention time is a complex function of both the retention ratio and the flow-rates, \dot{V}_c , \dot{V}_{out} and \dot{V}_{in} (ref. 7). At high retention degrees (low retention ratios) the retention time is constant for constant \dot{V}_c/\dot{V}_{out} or $\dot{V}_{in}/\dot{V}_{out}$ (ref. 7).

The relative zone broadening in flow FFF, *e.g.*, expressed as the observed average plate height, \bar{H} , or the plate number, N , should decrease as the retention ratio decreases if the non-equilibrium processes are the dominating zone broadening effects⁸. Zone broadening is also strongly dependent on the channel thickness, *i.e.*, it decreases as the channel is made thinner⁸, provided the retention ratio is constant. However, results published so far show that the observed plate height is much higher than expected, indicating that some "instrumental" zone broadening processes occur that have not been included in the zone broadening theory. Nevertheless, it should be worthwhile to decrease the channel thickness so as to produce more efficient separations.

In a normal, symmetrical flow FFF channel the resolution between two compounds will steadily increase when the cross-flow-rate is increased⁸, *i.e.*, when

retention increases. The separation can then be optimized by keeping the ratio of the cross-flow-rate to the channel flow-rate constant, while increasing the values of both⁸. This approach keeps the retention time constant while increasing the resolution. For rapid separations, a flow-rate ratio is chosen that gives a suitable retention time.

In the asymmetrical flow FFF channel a similar situation exists: the retention time is a function of the ratio \dot{V}_c/\dot{V}_{out} (ref. 7). When this ratio is kept constant the retention time remains constant. In the absence of a complete theory for the plate height and resolution in the asymmetrical channel, we optimized the separation speed and resolution empirically. A similar approach to that for a symmetrical channel was used, *i.e.*, the ratio \dot{V}_c/\dot{V}_{out} was chosen to give the desired retention times, while the value of $\dot{V}_{in} = \dot{V}_c + \dot{V}_{out}$ was increased to improve resolution.

It should be pointed out that the present asymmetrical flow FFF channel creates a linearly decreasing longitudinal velocity gradient down the channel⁷. The local non-equilibrium plate height, H , will therefore decrease along the channel's longitudinal axis, and the resulting average (or observed) plate height, $\bar{H} = L\sigma_t^2/t_R^2$ (where σ_t is the standard deviation of the peak in time units) will be a complex function of the flow-rates \dot{V}_c and \dot{V}_{out} . This effect will be dealt with in subsequent papers. The plate numbers presented below have been calculated from the observed average plate height, \bar{H} .

Proteins and aggregates

Figs. 1 and 2 show the separation of the monomer and the presumed dimer of the two proteins ferritin and thyroglobulin. These separations are of the same kind as already reported for albumin³ and were performed in the thicker channel (0.032 cm). The flow-rates were adjusted to give an elution time of 7 min for both monomers. Under these conditions they are highly retained, corresponding to about 40 and 50

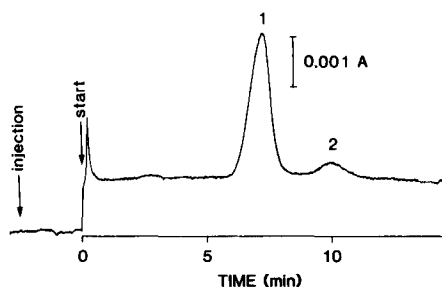
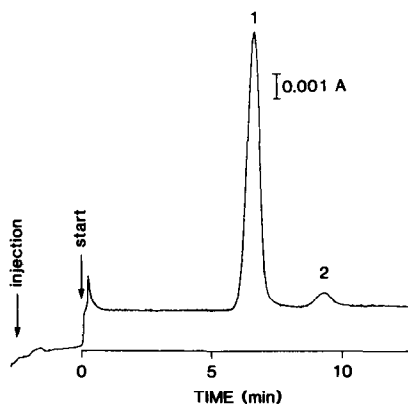


Fig. 1. Fractionation of ferritin (MW = 440 000) in channel I. Peaks: 1 = monomer; 2 = dimer. Sample: ferritin, 2 mg/ml, 10 μ l. Relaxation/focusing: $\dot{V}_c = 4$ ml/min, $z' = 4.3$ cm. Injection: flow-rate = 0.05 ml/min during 0.25 min and 0.02 ml/min during 1.75 min; loop volume = 10 μ l. Elution: $\dot{V}_c = 4.7$ ml/min, $\dot{V}_{out} = 2.4$ ml/min, $t_0 = 0.18$ min.

Fig. 2. Fractionation of thyroglobulin (MW = 669 000) in channel I. Peaks: 1 = monomer; 2 = dimer. Sample: thyroglobulin, 2 mg/ml, 10 μ l. Relaxation/focusing: $\dot{V}_c = 5$ ml/min, $z' = 4.2$ cm. Injection, as in Fig. 1. Elution: $\dot{V}_c = 3.7$ ml/min, $\dot{V}_{out} = 3.4$ ml/min, $t_0 = 0.15$ min.

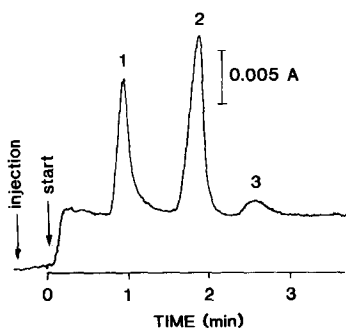


Fig. 3. Rapid separation of a protein mixture in channel II. Peaks: 1 = cytochrome *c*; 2 = albumin monomer; 3 = albumin dimer. Sample: cytochrome *c*, 10 mg/ml, 1 μ l; human serum albumin, 1.25 mg/ml, 9 μ l. Relaxation/focusing: $\dot{V}_c = 5$ ml/min during 1 min, and 9.9 ml/min during 15 s, $z' = 5$ cm. Injection: flow-rate = 0.1 ml/min, loop volume = 10 μ l, time = 1 min. Elution: $\dot{V}_c = 8.9$ ml/min, $\dot{V}_{out} = 0.8$ ml/min, $t_0 = 0.09$ min.

void times ($t_R/t_0 = 1/R$), respectively. The presumed dimers occur at about 50 and 70 void times, respectively. The high retention levels lead to the high resolution observed. The plate numbers for the monomer peaks are 840 and 340, respectively. When lower values for \dot{V}_c/\dot{V}_{out} were used, elution times were shorter at the cost of lower resolution.

Fig. 3 shows the separation of two proteins and a presumed dimer in the thin (0.012 cm) channel. Here, the ratio \dot{V}_c/\dot{V}_{out} was adjusted to give very rapid elution, and \dot{V}_{in} was raised to an high value to improve resolution. The plate numbers are 172 and 455, respectively, for peaks 1 and 2, while the retention levels correspond to about 10, 20 and 28 void times. When the same sample was studied in the thicker channel with the same short elution times, the resolution was much lower. These results appear very promising for rapid protein separations.

The identity of the presumed dimer peaks was not confirmed by other techniques but is supported by several observations. The proteins used are known to show aggregate peaks in SEC. Further, the ratio of the dimer peak retention time to the monomer peak retention time is constant, 1.40, for all three proteins, albumin, ferritin and thyroglobulin. For well retained components the retention time in asymmetrical flow FFF is inversely dependent on the component's diffusion coefficient⁷, D , which in turn depends on the component's molecular weight according to a simple power law⁸, $D = A/M^b$ (A is a constant, M is the molecular weight). The exponent b is 0.33 for a spherical particle and increases as the particle becomes more elongated⁸. The ratio 1.40 then corresponds to a value of $b = 0.49$ which does not seem unreasonable for a protein dimer.

One obvious application for flow FFF would be the detection of higher aggregates of proteins. Isocratic experiments like those represented by Figs. 1–3 would then result in very long retention times and considerable dilution of aggregates, making detection difficult. In such cases, the use of flow programming⁸ to decrease the ratio \dot{V}_c/\dot{V}_{out} would speed up the elution of the aggregates. Fig. 4 demonstrates such an experiment in the thicker channel. The ratio \dot{V}_c/\dot{V}_{out} was initially set very high to retain the low-molecular-weight end of the sample spectrum sufficiently long for the first peak to become relatively narrow. The ratio \dot{V}_c/\dot{V}_{out} was then decreased rapidly to a low value so that the presumed dimer and trimer were eluted relatively rapidly. In

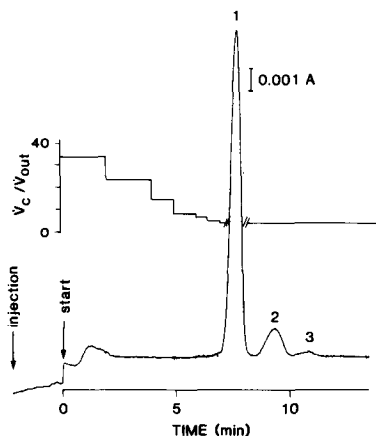


Fig. 4. Stepwise gradient elution of human serum albumin (HSA, MW = 67 000) in channel I. Peaks: 1 = monomer; 2 = dimer; 3 = trimer. Sample: HSA, 3 mg/ml, 10 μ l. Relaxation/focusing: $\dot{V}_c = 5$ ml/min, $z' = 4.2$ cm. Injection as in Fig. 1. Elution: $\dot{V}_c + \dot{V}_{out} = 7$ ml/min, decreasing \dot{V}_c/\dot{V}_{out} in six steps.

isocratic experiments the trimer was undetected due to the dilution. The fractogram in Fig. 4 should be compared with the isocratic experiment in Fig. 3 in our previous work³. By proper adjustment of the ratio \dot{V}_c/\dot{V}_{out} it should be possible to detect much larger aggregates.

Plasmids

Fig. 5 illustrates a model separation of two plasmids, differing in the number of base pairs by a factor of 1.8. The separation time is short and the resolution is more than adequate for many applications. The fractogram was obtained by using the thin channel: the plate numbers for both peaks are about 450. When the same separation was carried out in the thicker channel the resolution was incomplete (see also similar experiments in ref. 3). Optimization of the flow-rates with the thin channel resulted in much improved resolution and decreased separation time.

The small interfering responses close to peak 2 in Fig. 5 appear to be due to an heterogeneous composition of the plasmid pGL101 (peak 1). When this plasmid was

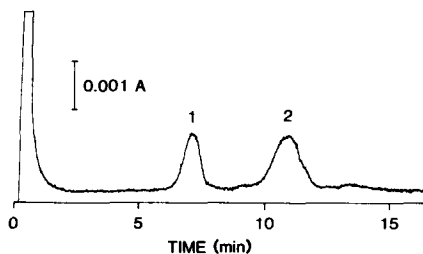


Fig. 5. Separation of the plasmids pGL101 (2390 base pairs) and pBR322 (4320 base pairs) in channel II. Peaks: 1 = pGL101, 0.1 μ g/ μ l, 1 μ l; 2 = pBR322, 0.1 μ g/ μ l, 1 μ l. Relaxation/focusing: $\dot{V}_c = 2$ ml/min, $z' = 4.2$ cm, time = 3 min. Injection: flow-rate = 0.1 ml/min, loop volume = 98 μ l, time = 2 min. Elution: $\dot{V}_c = 1.9$ ml/min, $\dot{V}_{out} = 0.6$ ml/min, $t_0 = 0.24$ min.

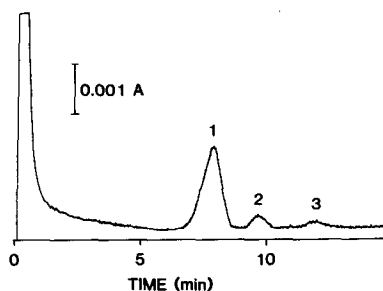


Fig. 6. Fractionation of the plasmid pGL101 (2390 base pairs) in channel II. Peaks: 1 = plasmid; 2 and 3 = possibly aggregates or conformational variants of the plasmid. Sample: pGL101, 0.1 $\mu\text{g}/\mu\text{l}$, 5 μl . Relaxation/focusing: $\dot{V}_c = 2 \text{ ml/min}$, $z' = 4.3 \text{ cm}$, time = 2 min. Injection: flow-rate = 0.05 ml/min, loop volume = 10 μl , time = 1 min. Elution: $\dot{V}_c = 1.6 \text{ ml/min}$, $\dot{V}_{\text{out}} = 0.42 \text{ ml/min}$, $t_0 = 0.32 \text{ min}$.

fractionated separately (see Fig. 6) two extra responses occurred. They may be due to aggregates or conformation variants of the plasmid pGL101 sample.

In the course of this study, we noted changes in the retention characteristics with sample load. These effects increased with the size of the plasmid, and were more pronounced in the thinner channel. The result of these effects was a tendency for peak fronting, and elution of a portion of the sample close to the void time. The effect is demonstrated by the differences between the two fractograms in Figs. 5 and 6. A possible explanation is that the highly concentrated sample zone formed during sample focusing creates an intermolecular repulsion which prevents the entire sample from relaxing to the correct equilibrium level above the accumulation wall. Thus, part of the sample would be relaxed too far away from the wall, resulting in early elution. The maximum sample size may be increased by allowing the sample to focus over a larger area of the ultrafiltration membrane.

Plasmid fragments

Separation of the fragments, obtained from plasmids after treatment with restriction enzymes, can be carried out rapidly with asymmetrical flow FFF³. Those cases where relatively few fragments occur seem best suited for the technique. In our previous study³ with a thick channel (0.03 cm), the separation of two fragments, one relatively small, the other big, was easily achieved. However the separation time was rather long (about 40 min) and the late-eluted big fragment gave a very broad band.

Stepwise flow programming can be used to speed up the elution of the large fragments in such work. This is demonstrated in Fig. 7, where the small fragment is eluted isocratically at a relatively high retention level, corresponding to about 22 void times. This contributes to an improved resolution for the small fragment. Then, the cross-flow-rate is reduced to zero in one step, resulting in immediate elution of the big fragment. The total separation time was 30 min, compared to 60 min in the previous work³. The sample applied was 16 μg .

Fig. 8 shows a rapid high-resolution separation of three "small" plasmid fragments (200, 700 and 1200 base pairs), performed in the thinner channel. The plate numbers for the three peaks are, respectively, 330, 580 and 1350, and the retention degree corresponds to *ca.* 13, 27 and 59 void times, respectively. All three fragments were eluted in about 0.5 ml of carrier. The thin channel has the advantage of giving

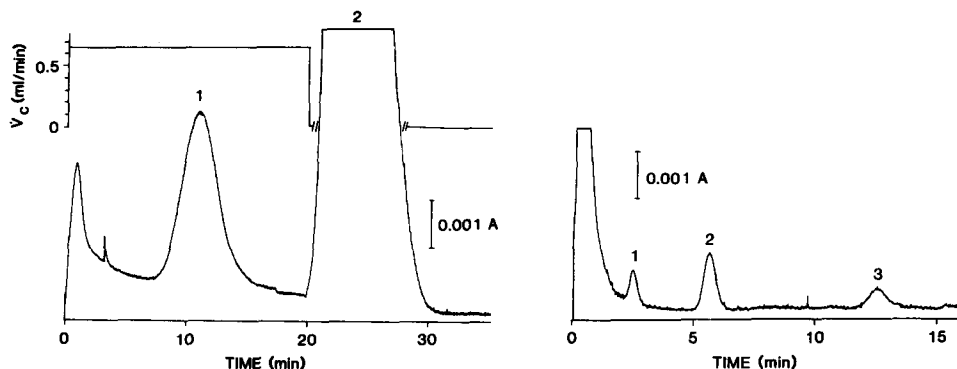


Fig. 7. Micropreparative separation of plasmid fragments with flow programming in channel I. Peaks: 1 = 700 base pairs (bp); 2 = 4600 bp. Sample: fragments from the plasmid pTL830 cleaved with PstI and BglII, 0.4 $\mu\text{g}/\mu\text{l}$, 40 μl . Relaxation/focusing, $\dot{V}_c = 4$ ml/min, $z' = 4.7$ cm, time = 8 min. Injection: flow-rate = 0.05 ml/min, loop volume = 10 μl , four loop volume were injected during 7 min. Elution: time = 0–20 min, $\dot{V}_c = 0.66$ ml/min, $\dot{V}_{\text{out}} = 1.2$ ml/min, $t_0 = 0.49$ min; time > 20 min, $\dot{V}_c = 0$ ml/min, $\dot{V}_{\text{out}} = 1.2$ ml/min.

Fig. 8. Separation of three plasmid fragments in channel II. Peaks: 1 = 200 bp, 0.01 μg ; 2 = 700 bp, 0.05 μg ; 3 = 1200 bp, 0.04 μg . The fragments were obtained from three different digests of the plasmid pTL830, each giving one big and one small fragment. The small fragments had previously been isolated in channel I. Sample volume = 700 μl . Relaxation/focusing: $\dot{V}_c = 4$ ml/min, $z' = 4.7$ cm, time = 7.5 min. Injection: flow-rate = 0.2 ml/min, loop volume = 98 μl , seven loop volume were injected during 6.5 min. Elution: $\dot{V}_c = 2.8$ ml/min, $\dot{V}_{\text{out}} = 0.5$ ml/min, $t_0 = 0.22$ min.

greater separation speed, resolution and smaller peak elution volumes. A disadvantage is the concentration effect noted for large fragments, similar to the large plasmids discussed above. This effect limits the sample sizes in preparative separations.

Viruses

The retention, separation and characterization of virus particles by flow FFF has already been studied⁹. However, the conditions used led to very long elution times, often several hours. In line with on-going efforts to develop rapid flow FFF separations^{3,8}, we now demonstrate such separations for viruses. Two viruses were studied, with molecular weights of *ca.* $1.8 \cdot 10^6$ and $50 \cdot 10^6$. Results are shown in Figs. 9 and 10. The cross-flow-rate in each case was chosen to give high retention levels (18 and 22 void times, respectively) which increases the resolution; the ratio $\dot{V}_c/\dot{V}_{\text{out}}$ was adjusted to give short elution times. The smaller virus (Fig. 9) was given an elution time of only 2.5 min while the larger virus was eluted at 5 min (Fig. 10). It should be pointed out that by proper change of the ratio $\dot{V}_c/\dot{V}_{\text{out}}$ any elution time can be chosen for a given component.

The virus peaks appear well shaped, but the smaller virus in Fig. 9 has a tendency to give a skewed peak, which may be caused by an heterogeneous composition of the sample (perhaps due to some aggregation). The peak from the larger virus shows a slight tail which may be caused by instrumental factors. The peak efficiency, as expressed by the plate number, N , is 242 and 590, respectively.

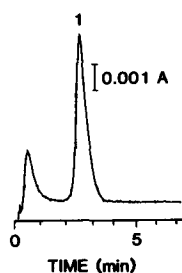


Fig. 9. Isolation of Satellite tobacco necrosis virus ($MW = 1.8 \cdot 10^6$) in channel II. Peaks: 1 = virus, $3 \mu\text{g}/\mu\text{l}$, $2 \mu\text{l}$. Relaxation/focusing: $V_c = 3 \text{ ml/min}$, $z' = 4.3 \text{ cm}$, time = 2 min. Injection: flow-rate = 0.05 ml/min , loop volume = $10 \mu\text{l}$, time = 1 min. Elution: $V_c = 4.35 \text{ ml/min}$, $V_{\text{out}} = 0.67 \text{ ml/min}$, $t_0 = 0.15 \text{ min}$.

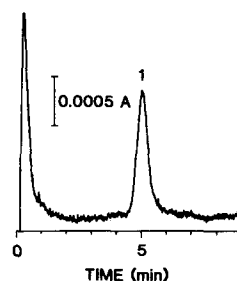


Fig. 10. Isolation of Semliki forest virus ($MW = 50 \cdot 10^6$) in channel II. Peaks: 1 = virus, $0.1 \mu\text{g}/\mu\text{l}$, $5 \mu\text{l}$. Relaxation/focussing: $V_c = 2 \text{ ml/min}$, $z' = 3.8 \text{ cm}$, time = 2 min. Injection: flow-rate = 0.1 ml/min , loop volume = $10 \mu\text{l}$, time = 0.5 min. Elution: $V_c = 1.65 \text{ ml/min}$, $V_{\text{out}} = 0.74 \text{ ml/min}$, $t_0 = 0.23 \text{ min}$.

ACKNOWLEDGEMENTS

Drs. L. Liljas and T. Unge (Department of Molecular Biology, University of Uppsala, Uppsala, Sweden) generously gave the samples of SFV and STNV, respectively. We are grateful for discussions with Professor B. Strandberg of the same Department. Dr. G. Swedberg (Department of Pharmaceutical Microbiology, University of Uppsala) generously supplied samples of plasmids and cleaved plasmids. Pharmacia Biotechnology generously gave plasmids, protein samples and instrument parts. This work was financially supported by the Swedish Natural Science Research Council.

REFERENCES

- 1 J. C. Giddings, *Sep. Sci.*, 1 (1966) 123.
- 2 J. C. Giddings, *Sep. Sci. Technol.*, 19 (1984–85) 831.
- 3 K.-G. Wahlund and A. Litzén, *J. Chromatogr.*, 461 (1989) 73.
- 4 J. C. Giddings, in J. C. Giddings, E. Grushka, *Adv. Chromatogr. (N.Y.)*, 20 (1982) 217.
- 5 J. Å. Jönsson and A. Carlshaf, *Anal. Chem.*, 61 (1988) 11.
- 6 A. Carlshaf and J. Å. Jönsson, *J. Chromatogr.*, 461 (1989) 89.
- 7 K.-G. Wahlund and J. C. Giddings, *Anal. Chem.*, 59 (1987) 1332.
- 8 K.-G. Wahlund, H. S. Winegarner, K. D. Caldwell and J. C. Giddings, *Anal. Chem.*, 58 (1986) 573.
- 9 J. C. Giddings, F. J. Yang and M. N. Myers, *J. Virol.*, 21 (1977) 131.